Molecular Crystals and Liquid Crystals
Publication details, including instructions for authors and subscription information:
http://www.tandfonline.com/loi/gmcl16

Dielectric Heating and Relaxations in Nematic Liquid Crystals

M. Schadt [a]
[a] Central Research Units, F. Hoffmann-La Roche & Co, Ltd., CH-4002, Basel, Switzerland
Version of record first published: 14 Oct 2011.

To cite this article: M. Schadt (1981): Dielectric Heating and Relaxations in Nematic Liquid Crystals, Molecular Crystals and Liquid Crystals, 66:1, 319-336

To link to this article: http://dx.doi.org/10.1080/00268948108072683

Mol. Cryst. Liq. Cryst., 1981, Vol. 66, pp. 319–336
0026–8941/81/6604–0319 $06.50/0

Printed in the U.S.A.

Dielectric Heating and Relaxations in Nematic Liquid Crystals

M. SCHADT

Central Research Units, F. Hoffmann-La Roche & Co., Ltd., CH-4002 Basel, Switzerland.

(*Received July 15, 1980*)

Novel experiments on dielectric heating were made to induce changes of temperature ΔT in nematic liquid crystal layers. Measurements of the dependence of ΔT on cell voltage, driving frequency, electrode spacings, external cell temperature and liquid crystal material parameters are correlated with molecular relaxation processes occurring in the frequency range 0–10 MHz. Temperature increases ΔT up to 40°C were achieved at low driving voltages in nematics belonging to two different liquid crystal classes which exhibit large positive static dielectric anisotropies. It could be shown that homeotropic wall alignment leads to a markedly different dependence of $\Delta T(\omega)$ in the vicinity of the cross-over frequency ω_c, of the lowest dielectric relaxation process, compared with unoriented or parallel aligned layers. The material requirements and limits for a possible application of dielectric heating in liquid crystal displays are discussed.

1 INTRODUCTION

A number of studies have been made on the low frequency dielectric relaxation[1] of nematic liquid crystals. Most of the experiments have concentrated on the first low frequency relaxation process which can be attributed to the hindered rotation of the long molecular axis around its short axis.[1,2,3] A few experiments performed in nematics with strong positive dielectric anisotropy have been reported showing that such materials exhibit at least one more relaxation occurring at higher frequencies.[4,5] Both relaxation processes can be described by a Debye type of relaxation.[4–6]

The question arose as to the extent of molecular relaxation processes leading to dielectric losses needed to increase the temperature of nematic layers and as to whether dielectric heating could be related quantitatively with the

Paper presented at the Eighth International Liquid Crystal Conference, Kyoto, Japan, June 30–July 4, 1980.

relaxation phenomena in the frequency range studied (0–10 MHz). Other questions of interest are the effects of liquid crystal material parameters on relaxation and on dielectric heating phenomena as well as the influence of cell wall alignment on dielectric heating. The present study should also give insight into the type of liquid crystal material and cell properties required to render dielectric heating applicable in liquid crystal displays increasing their temperature *in situ*, thus giving rise to shorter electro-optical response times and requiring lower heating power compared with external heating systems.

2 DIELECTRIC HEATING

In the following the increase of temperature will be derived occurring in a nematic layer upon the application of a high frequency voltage. It shall be assumed that the dielectric dispersions occurring in different frequency ranges in nematic liquid crystals can each be described by a single relaxation process with a relaxation time τ_n; the index n referring to the nth relaxation process. Then the frequency dependence of the dielectric properties of the nematic layer can be described by a complex dielectric constant $\varepsilon^*(\omega)$ if no overlapping of the relaxation processes is assumed; i.e.

$$\varepsilon^*(\omega) = \varepsilon'(\omega) + j\varepsilon''(\omega),$$

where

$$\varepsilon'(\omega) = \frac{(\varepsilon_s - \varepsilon_\infty)}{(1 + \omega^2\tau_n^2)} + \varepsilon_\infty$$

and

$$\varepsilon''(\omega) = \frac{(\varepsilon_s - \varepsilon_\infty)\omega\tau_n}{(1 + \omega^2\tau_n^2)} \tag{1}$$

are the respective real and imaginary parts of the Debye-type[6] of relaxation. ε_s and ε_∞ are the low (static) and the high-frequency dielectric constants of the respective diespersion region. The relaxation time $\tau_n = 1/\omega_n = 1/2\pi f_n$ can be determined from measurements of $\varepsilon'(\omega_n) = (\varepsilon_s + \varepsilon_\infty)/2$ in the nth dispersion region of $\varepsilon'(\omega)$. The frequency dependence of the dielectric losses leading to the heating of the nematic layer is given by $\varepsilon''(\omega)$ in Eqs. (1). Maximum losses are reached at the angular frequency ω_n. If one assumes the relaxation to be hindered by an activation energy E_n and if τ_n depends exponentially on temperature, τ_n becomes

$$\tau_n = \tau_0 \exp\left(\frac{E_n}{kT}\right), \tag{2}$$

$T = (T_e + \Delta T)$ being the temperature in the nematic layer determined by the increase of temperature ΔT due to dielectric heating and the external cell temperature T_e. For the power dissipated in the layer due to dielectric losses one obtains from Eqs. (1) and (2)

$$P = \left[\frac{V^2 A\varepsilon_0(\varepsilon_s - \varepsilon_\infty)}{d}\right] \times \left[\frac{\omega^2\tau_n}{(1 + \omega^2\tau_n^2)}\right] \tag{3}$$

where A = electrode area, d = thickness of the nematic layer and V = cell voltage (rms). If one takes into account heat losses Q_l through the cell electrode plates one obtains for the approximate heat Q_0 stored in the volume of the cell

$$Q_0 \approx Pt - Q_l \approx C\Delta T \tag{4}$$

where C is the average heat capacity of the cell which is primarily determined by the glass plates and to a small extent also by the LC-layer; t = dielectric heating time. If one assumes heat losses $Q_l \propto \Delta T$

$$Q_l \approx q_1 \Delta T t$$

follows, where q_1 is the specific heat conductivity of the cell plates. For temperature-increases $\Delta T \ll kT_e^2/E_n$—a condition which is practically always fulfilled in reality—follows from the expression for Q_l and Eqs. (3) and (4)

$$\Delta T = \left[\frac{V^2 A\varepsilon_0(\varepsilon_s - \varepsilon_\infty)}{d(C + q_1 t)}\right] \times \left[\frac{\tau_n\omega^2 t}{(1 + \omega^2\tau_n^2)}\right]. \tag{5}$$

Equation (5) is an approximation describing the increase of temperature ΔT in a cell comprising a nematic layer due to dielectric heating. Heat losses due to radiation are neglected in Eq. (5). Also neglected is lateral heat diffusion from dielectrically heated areas (segmented electrodes) into cell areas comprising no electrode pattern.

Equation (5) shows that stationary temperatures $T = (T_e + \Delta T)$ are established in the nematic layer for extended periods of dielectric heating. Two different frequency regions are of special interest in the stationary state ($t \to \infty$), namely

$$\Delta T\left(\omega \ll \frac{1}{\tau_n}\right) = \left[\frac{V^2 A\varepsilon_0(\varepsilon_s - \varepsilon_\infty)}{q_1 d}\right] \times \omega^2\tau_n \tag{6a}$$

$$\Delta T\left(\omega \gg \frac{1}{\tau_n}\right) = \left[\frac{V^2 A\varepsilon_0(\varepsilon_s - \varepsilon_\infty)}{q_1 d}\right] \times \tau_n^{-1}. \tag{6b}$$

Equation (6a) shows that the temperature increases as $\Delta T \propto \omega^2\tau_n$ at low frequencies. For $\omega \to \infty$ the increase of ΔT becomes independent of frequency reaching a maximum stationary value which increases with decreasing

relaxation time τ_n (Eq. 6b). In both regions ΔT depends on the square of the applied voltage, increasing linearly with decreasing electrode spacing d and increasing dielectric anisotropy $(\varepsilon_s - \varepsilon_\infty)$ respectively. Reducing the heat losses through the electrodes and/or the heat capacity of the electrode plates leads to an increase of the stationary temperature $T = (T_e + \Delta T)$ of the layer (c.f. Eqs. 6).

3 EXPERIMENTAL: RELAXATION BEHAVIOUR

The experiments were performed with two positive dielectric nematic binary mixtures containing components belonging to two distinctly different liquid crystal classes, namely the cyano alkyl Schiff' base mixture RO–TN–200 and mixture $M = (P_3 5, P_3 7)$ comprising the pentyl and heptyl cyano pyrimidines[7] $P_3 5$ and $P_3 7$ in molar proportions 40%:60%. Binary mixtures were chosen instead of single components because of their larger mesomorphic ranges thus allowing to perform measurements over a wider temperature range. As the alkyl chains of the homologous components in the respective mixtures differ at the most by three carbon atoms the relaxation behaviour of the mixtures can be assumed to be similarly uniform as that of the respective components.[5] The liquid crystal materials are from F. Hoffmann–La Roche.

The apparatus to measure the frequency dependence of the complex dielectric constants using magnetic fields to align the nematics was described earlier.[2] The measurements of the temperature $T = (T_e + \Delta T)$ in liquid crystal layers were made with tiny (80 μm) copper-constantan thermocouples. One of the soldering points of the couple was incorporated in one of the cell electrodes thus being in direct contact with the liquid crystal layer whereas the external cell temperature T_e of the thermostat was used as the reference temperature. The experimental arrangement allowed to detect temperature increases due to dielectric heating $\Delta T = (T - T_e) > 0.005°C$. To avoid Ohmic losses in the cell electrodes at high frequencies, stripes of silver electrodes with series resistivities < 2 Ohms and an active electrode area of 1 cm^2 were evaporated on 3 mm thick and 25 × 30 mm large glass plates. Electrode spacings between 12 μm and 50 μm were chosen.

Angular evaporation of SiO onto the silver electrodes was used to obtain parallel wall alignment with zero bias tilt angles. To achieve homeotropic boundaries a 60 Å thick layer of SiO_x was evaporated onto the silver electrodes which was then coated with a layer of silane. The uniformity of the respective wall alignments were checked by capacitance measurements of the full cells.

Figure 1 shows measurements of the frequency- and temperature dependence $\varepsilon_{\parallel}(\omega, T)$ as well as the (frequency independent) temperature dependence of the static dielectric constant $\varepsilon_{\perp}(T)$ of RO–TN–200. The cross-over frequency f_c denotes the frequency at which the rotation of the long molecular axis around the short axis becomes hindered to such an extent that the redistribution of the dipole moments parallel to the long axis leads to $\varepsilon_{\parallel}(T, f = f_c) = \varepsilon_{\perp}(T)$. For frequencies $f > f_c$ the dielectric anisotropy $\Delta\varepsilon(\omega) = (\varepsilon_{\parallel}(\omega) - \varepsilon_{\perp})$ changes sign. The intersections between the lower dashed graph in Figure 1 and the measurements of $\varepsilon_{\parallel}(\omega, T)$ indicate the values where $\varepsilon_{\parallel}(\omega, T) = \varepsilon_{\perp}(T)$ was measured. From the projections of these intersections onto the abscissa follows $f_c(T)$. Also plotted in Figure 1 are the frequencies for which $\varepsilon_{\parallel}(f = f_1) = (\varepsilon_s + \varepsilon_{\infty})/2$ (upper dashed graph), where $\varepsilon_{\parallel} = \varepsilon_s \cdot f_1$ corresponds to the lowest relaxation time τ_1 of the first hindered rotation[4] around the short molecular axis.

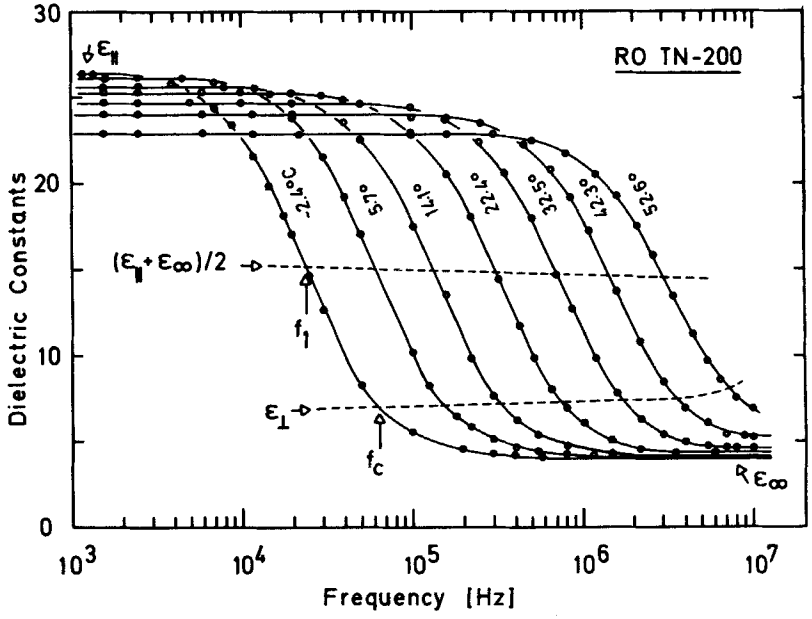

FIGURE 1 Measured frequency- and temperature dependence of the parallel ($\varepsilon_{\parallel}$) and perpendicular ($\varepsilon_{\perp}$) dielectric constants of RO–TN–200.

Figure 2 shows the temperature dependence of f_c and τ_2 of RO–TN–200 derived from the measurements in Figure 1. From the representation in Figure 2 follows that both material properties exhibit an exponential temperature dependence with activation energies $E_1 \simeq E_c = 0.67$ eV. This

finding verifies the assumptions made in paragraph 2 that at least the first relaxation process depends exponentially on temperature and can be described by a single relaxation time τ_1.

It was shown earlier that at least one more relaxation process occurs in the liquid crystal materials and frequency range investigated here.[4,5] The relaxation time τ_2 corresponding to the second dispersion region lying at higher frequencies could not be determined from dielectric relaxation measurements. However, as shown before[4] it is possible to determine τ_2 from measurements of the frequency dependence of the specific conductivity

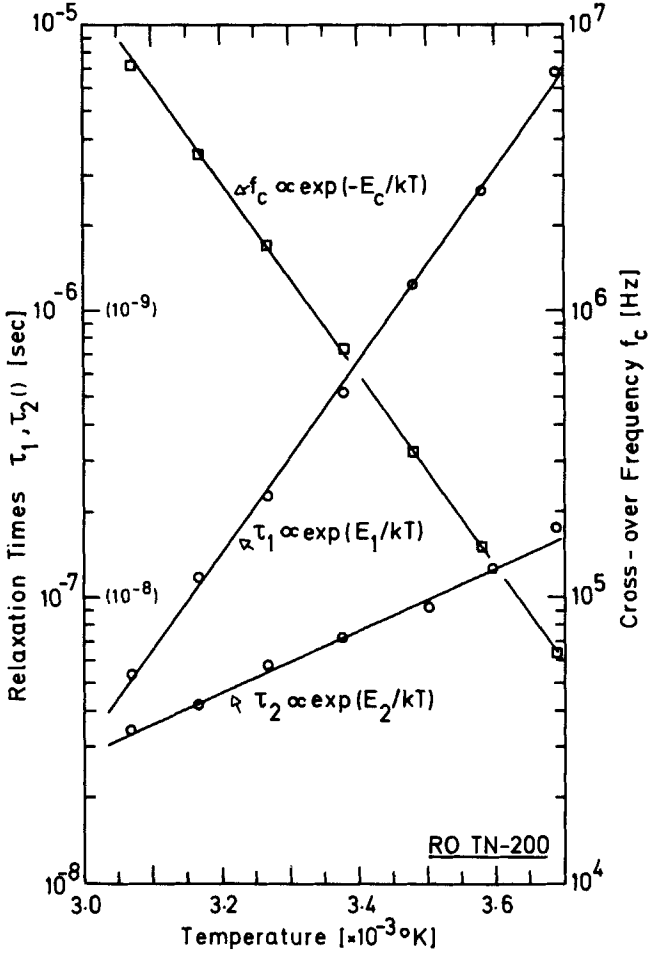

FIGURE 2 Measured temperature dependence of the cross-over frequency f_c and the relaxation times τ_1 and τ_2 of RO-TN-200.

$\sigma_\perp(\omega, T)$ in the dispersion region of the respective orientation polarization. For frequencies $\omega\tau_2 \ll 1$ and conductivities $\sigma_\perp(\omega) \gg \sigma(\text{dc})$

$$\sigma_\perp(\omega) = \varepsilon_0(\varepsilon_\perp - 1)\tau_2\omega^2 \tag{7}$$

holds.[4,5] Thus, the relaxation times in the high frequency dispersion region were determined from measurements of $\sigma_\perp(\omega, T)$ together with the data for $\varepsilon_\perp(T)$ in Figure 1 using Eq. (7). The results are depicted in Figure 2. In analogy to $\tau_1(T)$ an exponential temperature dependence was found which can be described by a single relaxation time $\tau_2(T)$ and an activation energy $E_2 = 0.215$ eV (Figure 2). The dependence of τ_2 on temperature is considerably smaller than that of τ_1 which is reflected by $E_2 \simeq E_1/3$.

Table I shows the static and high frequency dielectric constants, the specific high frequency conductivities $\sigma_\perp$ and the frequencies f_1 and f_c of RO–TN–200 and mixture M measured at 22.1°C. Also shown are the respective relaxation times determined from these data and the activation energies for RO–TN–200. Due to its rather small mesomorphic range the temperature dependencies $\varepsilon(\omega)$ and $\sigma_\perp(\omega)$ of mixture M were not measured, thus the respective activation energies were not determined either. However, previous measurements reported for the temperature dependence of the relaxation of single pyrimidine components[5] indicate that—analogously to RO–TN–200—$E_2 < E_1 \simeq 0.62$ eV holds; this value for E_1 is depicted in Table I. The relaxation times of mixture M—especially τ_1—are shorter compared with those of RO–TN–200. This finding exhibits the same trend as the respective bulk viscosities η of the two mixtures (Table I).

4 DIELECTRIC HEATING; RESULTS

A Cells with no wall alignment

The measurements of dielectric heating effects in nematic layers described in this paragraph were all made in a quasi stationary manner; i.e. the changes of temperature measured correspond to $\Delta T = \Delta T(t \to \infty)$. To show the influence of wall alignment on $\Delta T(\omega, V)$ the measurements were made in unoriented as well as in parallel and homeotropically aligned cells. Except for the measurements made to verify the proportionality of ΔT on reciprocal electrode spacing d (c.f. Eq. 6) all experiments were performed with electrode spacings $d = 15\ \mu\text{m} + 0.5\ \mu\text{m}$. This spacing was chosen because it is comparable to those used in liquid crystal displays. The time required for ΔT to reach 90% of its stationary value $\Delta T(t \to \infty)$ after applying a high frequency driving voltage depends strongly on the heat losses and electrode and plate

geometries of the cells (c.f. Eq. 6). With $d = 15\ \mu m$ and the rather bulky glass plates of the cells used here, this time was typically 100 seconds.

Figure 3 shows measurements of the dependence of ΔT on cell voltage and driving frequency performed in cells with no wall alignment and at constant external temperature $T_e = 22.1°C$ using RO–TN–200. The dashed graph shows the temperature dependence of the cross-over frequency $f_c(T = T_e + \Delta T)$ following from the relaxation measurements depicted in Figure 2. The measurements in Figure 3 show that considerable temperature increases can be achieved by dielectric heating at rather low driving voltages. At low cell voltages two distinct dispersion regions where $\Delta T(V = \text{const.}) \propto \omega^2$ were found (Figure 3) which are separated at intermediate frequencies by a pronounced maximum ΔT_{max} of the graphs $\Delta T(f, V = \text{const.})$. The frequency at

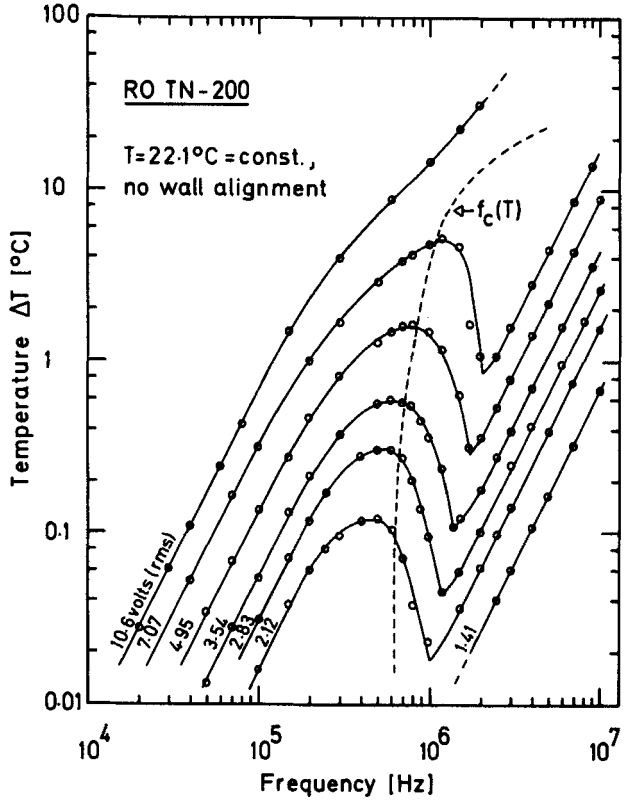

FIGURE 3 Measured dependence of the increase of temperature ΔT versus driving frequency and cell voltage due to dielectric heating of RO–TN–200. The external cell temperature was 22.1°C = constant; no wall alignment was used; electrode spacing $d = 14.5\ \mu m$. The dashed graph shows the dependence of the cross-over frequency f_c on the temperature of the nematic layer determined separately from dielectric relaxation measurements.

TABLE I

Measurements made at $T = 22.1°C$ = constant using mixtures RO–TN–200 and $M = (P_35, P_37)$ respectively. T_c = nematic–isotropic transition temperature, η = bulk viscosity, $\varepsilon_{\parallel}$ and $\varepsilon_{\perp}$ are the static dielectric constant measured at $f \gg f_c$ = cross-over frequency, $\sigma_{\perp}$ = specific conductivity measured perpendicular to the nematic director at $f = 1$ MHz, τ_1 and τ_2 and E_1 and E_2 are the relaxation times and the activation energies in the low and high frequency dispersion region respectively, $f_1 = f[(\varepsilon_{\parallel} + \varepsilon_{\infty})/2]$, $\Delta T(f = f_c)$ = increase of temperature in the nematic layers due to dielectric heating at the driving frequency $f = f_c$ and at constant voltage $V = 4.95$ volts using unoriented cells with electrode spacinds $d = 15$ μm.

LC	T_c [°C]	η [cp]	$\varepsilon_{\parallel}$ (1.6kHz)	$\varepsilon_{\perp}$ (1.6kHz)	ε_{∞} (10MHz)	$\sigma_{\perp}$ (1MHz) [$\Omega^{-1}m^{-1}$]	τ_1 [sec]	τ_2 [sec]	f_1 [MHz]	f_c [MHz]	E_1 [eV]	E_2 [eV]	$\Delta T(f=f_c)$ [°C]
RO–TN–200	65.8	84	25.29	7.36	4.30	1.6×10^{-5}	5.2×10^{-7}	7.2×10^{-9}	0.31	0.73	0.672	0.215	1.6
M=($P_3$5, $P_3$7)	50.6	52	31.70	7.20	4.28	1.1×10^{-5}	1.5×10^{-7}	5.1×10^{-9}	1.10	2.60	~0.62	——	~12

which ΔT_{max} is reached depends on temperature and corresponds with $f_c(T)$. The pronounced temperature maximum followed by a decrease of ΔT when increasing $f \gtrsim f_c$ disappears only at large temperatures where a strong increase of $f_c(T)$ with increasing temperature occurs (c.f. graph $\Delta T(V = 10.6$ volts in Figure 3)).

It will be shown that the dielectric heating mechanism in the low frequency dispersion region can be attributed to the hindered homeotropic reorientation of the long molecular axes around their short axes. At frequencies $f \ll f_c$ where $\Delta\varepsilon > 0$ the long molecular axes align parallel to the applied electric field. In agreement with Eq. (6a) $\Delta T \propto \omega^2$ holds in this frequency range (Figure 3). Increasing the frequency further causes $\Delta\varepsilon(f) > 0$ to decrease until $\Delta\varepsilon(f = f_c) = 0$ is reached. For $f \gtrsim f_c$ the dielectric anisotropy changes sign thus causing a reorientation of the long molecular axes from the homeotropic into an alignment parallel to the cell electrodes. As a consequence the relaxation mechanism governing the dielectric heating process in the low frequency region ceases to exist thus leading to a decrease of

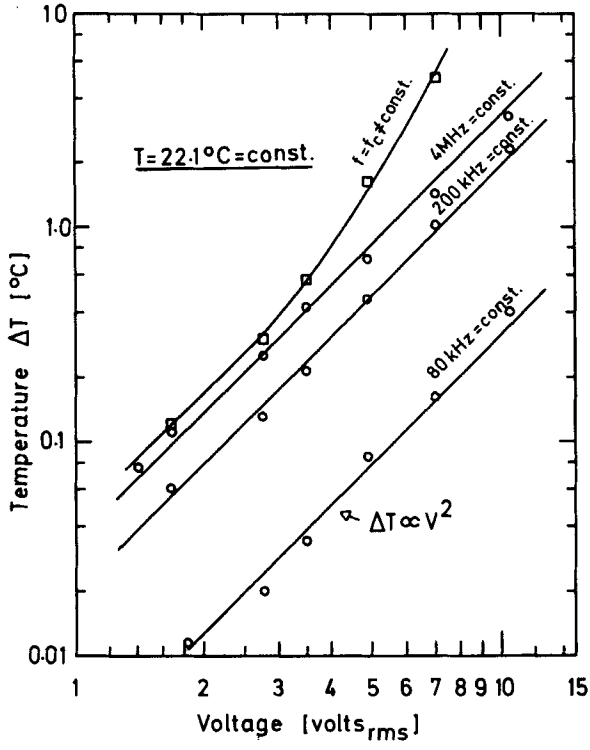

FIGURE 4 Dependence of ΔT on cell voltage measured at different frequencies at constant external cell temperature (22.1°C) using RO–TN–200.

$\Delta T(f \gtrsim f_c)$ (Figure 3). Figure 3 shows that increasing the driving frequency further ($f \gg f_c$) causes ΔT to rise again with $\Delta T \propto \omega^2$, indicating that a second dispersion region is entered. The dependence $\Delta T \propto \omega^2$ in this high frequency relaxation region is also in agreement with Eq. (6a) if it is assumed that $\omega \ll 1/\tau_2$. The dielectric anisotropy in this region is $(\varepsilon_s - \varepsilon_\infty) \simeq (\varepsilon_\perp - \varepsilon_\infty) \simeq$ constant. The measurements $\Delta T(V = 10.6$ volts) in Figure 3 indicate that the second dispersion region cannot be reached if dielectric heating in the low frequency dispersion region causes $f_c(T)$ to increase to such an extent that the graphs $\Delta T(f, V)$ cease to intersect the dashed graph $f_c(T)$. In this case f_c escapes so to say and the nematic layer does not reach the condition $\Delta\varepsilon(f > f_c) < 0$ which seems to be a prerequisite for entering the second dispersion region.

The measurements depicted in Figure 4 are derived from those of Figure 3 and show the dependence $\Delta T \propto V^2$ predicted by Eq. (5) to hold in both, the low and the high frequency dispersion region. Due to the shift of f_c towards

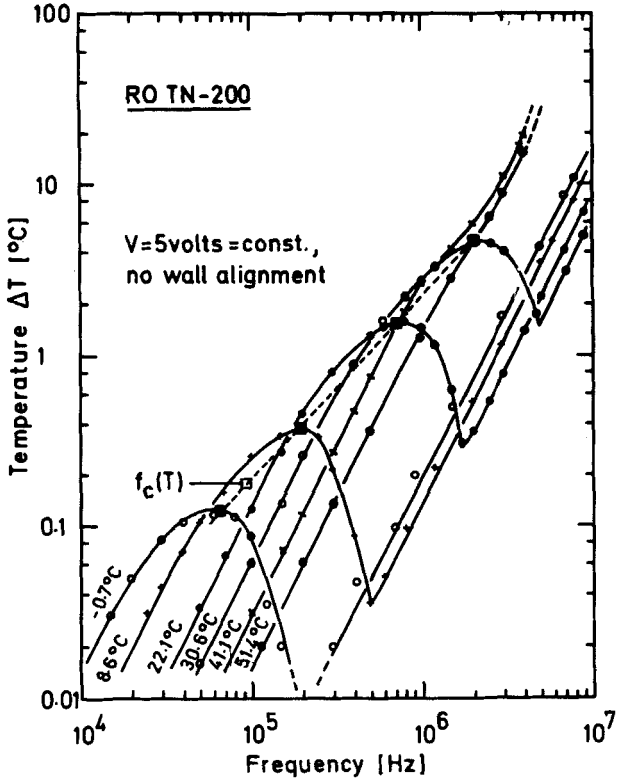

FIGURE 5 Dependence of ΔT of RO–TN–200 on external cell voltage measured at constant driving voltage $V = 5$ volts. Electrode spacing $d = 14.5$ μm; no wall alignment.

higher frequencies with increasing driving voltage which leads to a strong increase of temperature in the nematic layer the square-law dependence no longer holds for $\Delta T(f = f_c \neq \text{const.})$ with increasing voltage (Figure 4).

Figure 5 shows measurements of the dependence of ΔT on external cell temperature T_e made at constant voltage using RO–TN–200. The projections of the black squares onto the abscissa that are plotted at the maxima of $\Delta T(f)$ are values of the cross-over frequencies $f_c(T)$ following from the relaxation measurements depicted in Figure 2. The graphs in Figure 5 show that $\Delta T(T_e) \propto \omega^2$ depends for $f < f_c$ much more on temperature than in the high frequency dispersion region. As a consequence a shift of the low frequency dispersion region to the latter occurs with increasing temperature T_e. $\Delta T(T = \text{const.}, V = \text{const.}) \propto \omega^2$ was found to hold in both dispersion regions over the whole temperature range studied (Figure 5).

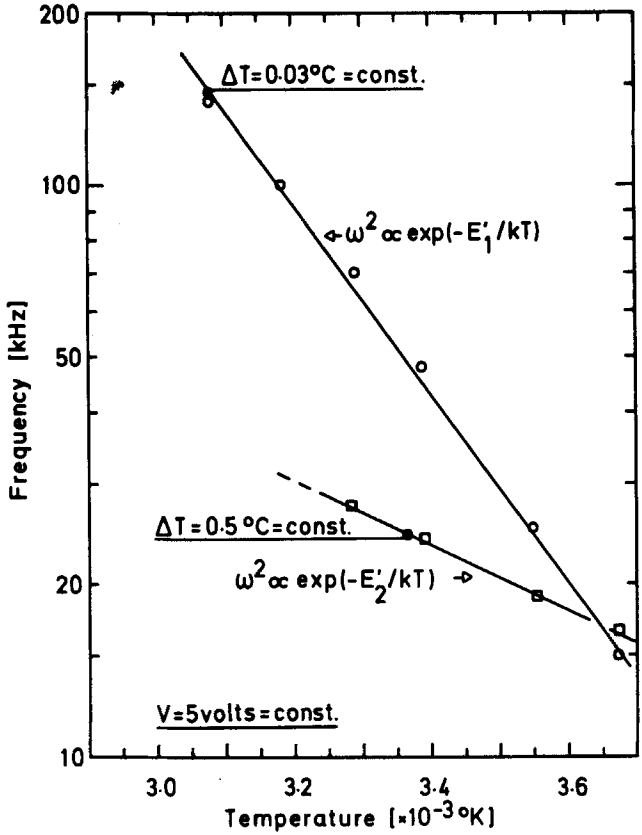

FIGURE 6 Dependence of angular driving frequency ω on external cell temperature of RO–TN–200 on condition that ΔT = const. and V = 5 volts = const., measured in the low- and high frequency dispersion region respectively.

From the measurements in Figure 5 follows for constant driving voltage the dependence of driving frequency on temperature T_e on condition that the increase of temperature ΔT remains constant; i.e. $\Delta T(f, T_e, V = \text{const.}) = \text{constant}$. This dependence determined in the two dispersion regions where $\Delta T \propto \omega^2$ holds is depicted in Figure 6. From Figure 6 follows $\omega^2 \propto \exp(-E'_n/kT)$ with the respective activation energies $E'_1 = 0.658$ eV and $E'_2 = 0.229$ eV. The energies E'_1 and E'_2 correspond within 5% with the energies E_1 and E_2 of the relaxation times τ_1 and τ_2 determined from the relaxation measurements (Table I). The results agree well with the frequency and with the temperature dependence following from Eqs. (2) and (6a).

The above findings clearly indicate that the same mechanisms leading to the relaxation behaviour described in Section 3 also govern the dielectric heating processes. They also show—together with the results following from the measurements depicted in Figures 3 and 4 and from those described below, using a different liquid crystal material—that the formalism derived in Section 2 can be used to describe dielectric heating in unoriented nematic layers quantitatively over most of the frequency range studied.

To get an impression as to what extent a different liquid crystal class with different physical properties (Table I) influences the dielectric heating processes in unoriented cells, the strongly positive dielectric pyrimidine mixture M was also investigated. Figure 7 shows measurements of the frequency— and voltage dependence of ΔT at constant external cell temperature T_e using mixture M. The same cells were used as for the experiments made with RO–TN–200. The graphs in Figure 7 show a dependence analogous to that found for RO–TN–200 (Figure 3). However, due to the lower relaxation time τ_1 of mixture M (Table I) the first dispersion region is shifted towards higher frequencies. Besides, comparing graphs measured at the same cell voltage in Figures 3 and 7 shows that considerably higher temperature increases ΔT_{max} are reached in the first dispersion region when using mixture M instead of RO–TN–200 (c.f. also last column in Table I). This finding is qualitatively in agreement with Eq. (5) and corresponds to the larger dielectric anisotropy $(\varepsilon_s - \varepsilon_\infty)$ and the shorter relaxation time τ_1 of mixture M (Table I).

To check the dependence of ΔT on material specific changes of $(\varepsilon_s - \varepsilon_\infty)$ and τ_1 respectively, the ratio $R = \Delta T$ (RO–TN–200)/$\Delta T(M)$ was calculated in the low frequency dispersion region using Eq. (6a). With $(\varepsilon_s - \varepsilon_\infty) = 20.99$ and 27.42 and the respective relaxation times $\tau_1 = 5.2 \times 10^{-7}$ sec and 1.5×10^{-7} sec (Table I) $R = 2.65$ was obtained. R compares well to the experimentally determined ratio $R_m = 2.50$ following from the respective measurements made at 100 kHz (Figures 3 and 7).

At this point it seems interesting to estimate the input power required to drive a cell with an electrode-area $A = 1\ \text{cm}^2$ and spacing $d = 15\ \mu\text{m}$ filled with RO–TN–200. For the cells used here $\Delta T = 30°\text{C}$ was obtained

when applying $V = 10.6$ volts at $T_e = 22°C$ and $f = 2$ MHz (Figure 3). Under these conditions it follows for the cell capacitance $C \simeq 1000$ pF thus the power required becomes $P \simeq 2.8$ Watts. Considering the thermally poorly designed cells used here it seems likely to achieve either considerably larger temperature increases ΔT or a reduction of the power requirements < 1 Watt/cm^2.

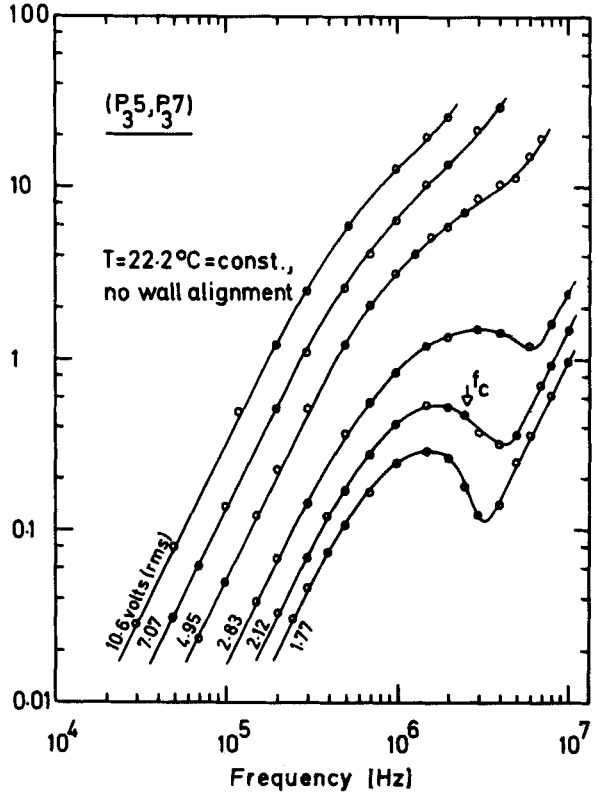

FIGURE 7 Frequency and voltage dependence of ΔT using pyrimidine mixture $M = (P_3 5, P_3 7)$ measured at constant external temperature in unoriented cells with an electrode spacing $d = 15.0\ \mu$m. f_c indicates the respective cross-over frequency determined from dielectric relaxation measurements.

B Cells with parallel and homeotropic wall alignment

If dielectric heating was to be applied in liquid crystal displays one would—depending on the specific electro-optical effect used—probably work with either homogeneous or homeotropic wall alignment. To show the influence

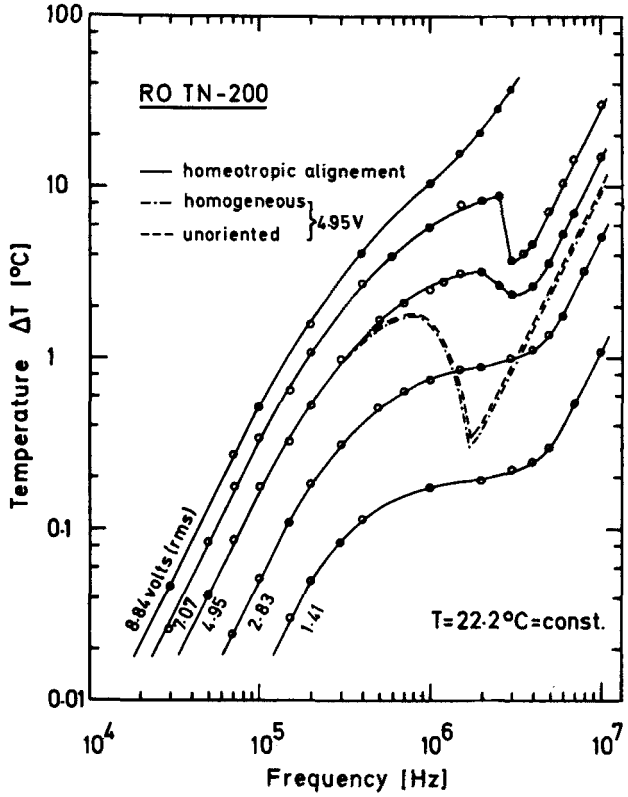

FIGURE 8 Dependence of ΔT on voltage and driving frequency measured in cells with homeotropic wall alignment ($d = 14.5\ \mu m$) at constant external cell temperature using RO–TN–200 (solid lines). The dashed graphs show the dependence of ΔT on frequency measured at constant driving voltage $V = 4.95$ volts using unoriented and cells with parallel wall alignment respectively.

of these two types of wall alignment on dielectric heating, measurements were made in parallel and homeotropically aligned cells respectively.

Figure 8 shows the dependence of ΔT on voltage and driving frequency measured in cells with homeotropic wall alignment at constant external temperature using RO–TN–200. Besides, Figure 8 shows measurements made in unoriented and parallel aligned cells respectively (dashed graphs; $V = 4.95$ volts = constant). Unoriented and parallel aligned cells led to virtually identical results at all cell temperatures and voltages used. (The voltages used were larger than the voltage $V_t \sim 0.7$ volts of the Fréedericksz transition in parallel aligned cells.) However, a markedly different dependence of $\Delta T(f, V)$ was found at frequencies between the low- and high-frequency

dispersion region when using homeotropic wall alignment (Figure 8). The measurements in Figure 8 show that homeotropic boundaries lead to an apparent shift of the cross-over frequencies f_c towards higher values f_c' as well as to larger maximum temperature increases ΔT_{max} at the high frequency end of the first dispersion region (Figure 8). The maximum of $\Delta T(f)$ found in unoriented cells at $\Delta T(f \simeq f_c)$ followed by a less pronounced decrease of ΔT for $f \gtrsim f_c'$ occurred only at larger voltages (Figure 8).

This behaviour is likely to be due to boundary layers of nematic molecules remaining at least partly homeotropically aligned in the vicinity of the electrodes at frequencies $f > f_c$. Contrary to the molecules in the centre between the electrodes which are much less affected by wall alignment forces and which therefore realign parallel for $\Delta\varepsilon(f > f_c) < 0$, the boundary layers maintain at least partly their homeotropic alignment for $f > f_c$. As a consequence only the centre molecules cease to contribute to the dielectric heating at frequencies $f > f_c$ whereas the boundary layers still contribute to the relaxation and the dielectric heating process governing the first dispersion region. Thus, the decrease of $\Delta T(f \gtrsim f_c)$ found in unoriented and parallel aligned cells respectively disappears at low voltages in homeotropically aligned cells. The decrease becomes only apparent at larger voltages because there the electric reorienting forces for $f \gtrsim f_c'$ increase (Figure 8).

As no residual homeotropic boundary layers exist in parallel aligned cells at frequencies $f > f_c'$ such cells exhibit a dielectric heating behaviour analogous to the one found in unoriented cells.

CONCLUSIONS

It could be shown that considerable increases of temperature in layers of positive dielectric nematic molecules can be achieved by applying medium to high frequency driving voltages to the cell electrodes. From measurements of the dielectric and polarization relaxation in two different nematic materials in the frequency range 0–10 MHz a low and a high frequency dispersion region was found. The relaxation process in each region could be described by the respective single relaxation times τ_1 and τ_2 depending exponentially on temperature. The potential energies determining the degree of hindrance of the respective relaxations were found to differ considerably; i.e. $E_1 \simeq 3E_2$. Thus, the dependence of the low frequency relaxation time τ_1 was considerably larger than that of τ_2. Besides, the former seems to be much more strongly influenced by class specific properties of different liquid crystal materials.

The low frequency relaxation leads with increasing frequency to a change

of the field-induced homeotropically aligned distribution $\hat{\mu}_\uparrow \neq \hat{\mu}_\downarrow$ of the permanent dipole moments $\hat{\mu}_\parallel$ into the field-free equilibrium state $\hat{\mu}_\uparrow = \hat{\mu}_\downarrow$. This relaxation is due to the strongly hindered reorientation of the permanent dipole moments $\hat{\mu}_\parallel$—lying parallel to the long molecular axes—around their short axes. The experiments showed that above the cross-over frequency f_c where the dielectric anisotropy changes sign from $\Delta\varepsilon(f < f_c) > 0$ to $\Delta\varepsilon(f > f_c) < 0$, dielectric heating due to the above relaxation ceases. This behaviour could be attributed to the reorientation of the long molecular axes from homeotropic to parallel alignment at $f \geqslant f_c$. The high frequency relaxation occurring at $f \geqslant f_c$ was earlier attributed to the hindered rotation of the short molecular axes around their long ones.[4, 5] Now the dielectric heating experiments seem to indicate that the high frequency relaxation may also be due to a hindered fluctuation of the long molecular axes around their short axes. The major difference between the low and the high frequency relaxation mechanism would thus consist in the different directions along which the long molecular axes align in the two frequency regions; i.e. $\hat{\mu}_\parallel(f < f_c) \| \hat{F}$ and $\hat{\mu}_\parallel(f > f_c) \perp \hat{F}$, where $\hat{F}$ is the applied electric field. This model makes the finding $E_1 \gg E_2$ plausible because the reorientation into the homeotropic alignment at frequencies $f < f_c$ is likely to be much more strongly hindered than the much smaller fluctuations of the long molecular axes around their short ones at frequencies $f > f_c$.

The dependence of the increase of temperature ΔT occurring in nematic liquid crystal layers due to dielectric heating on cell voltage, driving frequency, temperature, liquid crystal material properties and properties of the cells used was measured and quantitatively related to the respective molecular relaxation processes. The experiments were performed in unoriented as well as in cells with parallel and homeotropic wall alignment respectively. The measurements made in cells with homeotropic boundaries lead to larger increases of $\Delta T(f = f_c)$ compared with unoriented or homogeneously aligned cells. This finding could be attributed to dielectric heating effects of residual boundary layers that—due to forces exerted onto the molecules by the homeotropic wall alignment—remain at least partly homeotropically aligned at frequencies $f > f_c$.

The results reported indicate the possibility that dielectric heating may be applicable to improve the electro-optical response behaviour of liquid crystal displays at low temperatures. However, transparent electrodes with low conductivity, relatively large driving frequencies and liquid crystal materials with appropriate activation energies and relaxation times will be required. Then it seems for instance possible to apply dielectric heating to twisted nematic displays in the on- or off-state respectively, depending on whether a driving frequency $f < f_c$ (homeotropic alignment) or $f > f_c$ (homogeneous alignment) is used.

Acknowledgement

I wish to thank Dr. P. Gerber for very helpful discussions and would like to gratefully acknowledge the assistance of B. Blöchliger in the performance of the experiments.

References

1. W. Maier and G. Meier, *Z. Nat. Forsch.*, **16a**, 1200 (1961).
2. M. Schadt, *J. Chem. Phys.*, **56**, 1494 (1972).
3. D. Diguet, F. Rondelez, and G. Durand, *C.R. Acad. Sci. Ser.*, **B271**, 954 (1970).
4. M. Schadt and C. von Planta, *J. Chem. Phys.*, **63**, 4379 (1975).
5. M. Schadt, *J. Chem. Phys.*, **67**, 210 (1977).
6. P. Debye, *Polar Molecules* (Dover Publications, Inc. 1929).
7. A. Boller, M. Cereghetti, M. Schadt, and P. Scherrer, *Mol. Cryst. Liq. Cryst.*, **42**, 215 (1977).